Examining the Relative Motion of Derecho- and Non-Derecho-Producing QLCSs with Respect to the Mean Wind

MATTHEW A. CAMPBELL
National Weather Center Research for Undergraduates, Norman, Oklahoma
The Ohio State University, Columbus, Ohio

ARIEL E. COHEN
NOAA/NWS/NCEP/Storm Prediction Center, Norman, Oklahoma
University of Oklahoma School of Meteorology, Norman, Oklahoma

ANDY R. DEAN
Storm Prediction Center, Norman, Oklahoma

STEPHEN F. CORFIDI
Storm Prediction Center, Norman, Oklahoma

MICHAEL C. CONIGLIO
NOAA/National Severe Storms Laboratory, Norman, Oklahoma

SARAH J. CORFIDI
Cooperative Institute for Mesoscale Meteorological Studies, University of Oklahoma, Norman, Oklahoma

COREY M. MEAD
Storm Prediction Center, Norman, Oklahoma

_____
Corresponding author address: Matthew A. Campbell, The Ohio State University Department of Geography, 1036 Derby Hall, 154 North Oval Mall, Columbus, OH 43210.
E-mail: campbell.1635@osu.edu

Abstract

Since the term “derecho” was defined, vast technological and societal changes have taken place. Impactful developments include (1) the implementation of the WSR-88D radar network nationwide, which helps provide a structural view of mesoscale convective systems (MCSs), and (2) modern reporting practices which now provide substantially more severe-wind reports than in the past. These changes have caused the term “derecho” to become misapplied over the years, which has led to recent endeavors to refine the definition. This study aims to help clarify the term “derecho” by investigating relationships between radar-implied structural features of MCSs and the mean wind and propagation components of MCS motion. Results show that there is a correlation; specifically, well-organized MCSs move faster and have more propagation in the direction of mean wind than less organized systems. By understanding the relationship between MCS structure and motion, the process of MCS and derecho classification can incorporate physical features and motion of MCSs, in addition to wind-damage swaths, into the classification process.

1. Introduction

Organized clusters of thunderstorms with specific structural, thermodynamic, and kinematic characteristics can be classified as mesoscale convective systems (MCSs, e.g., Maddox et al. 1980; Parker 2000). MCSs produce a large amount of the annual summer rainfall in the middle latitudes of the United States, and their associated precipitation is often accompanied by a wide range of severe weather threats, including flooding, tornadoes and damaging winds (Jirak and Cotton, 2007). On top of contributing a large amount of warm-season rainfall throughout the central United States, MCSs also are responsible for a large portion of the severe weather cases in the central United States (Corfidi 2003, Fritsch et al. 1986), the most destructive and impactful of which can be severe straight-line winds that can reach hurricane force (Ashley and Mote, 2005).

The highest-impact and strongest severe-wind-producing MCSs are often classified as derechos (e.g., Cohen et al. 2007; Ashley and Mote 2005). These systems comprise up to forty percent of thunderstorm wind casualties caused by MCSs (Metz and Bosart 2010), while only compromising a small percentage of total MCSs. However, classification requirement issues, such as minimum damage swath length and wind strength, arise in the modern-day classification scheme for severe MCSs and derechos, which relies heavily on damage reports and surface observations that, in the past, tended to be relatively low in number. In modern times, the number of daily damage reports has grown significantly, which carries inherent drawbacks. Modern reports often have questionable reliability caused by unequal population distribution, inconsistent reporting and lack of measured observations due to gaps in the United States observation network (Weiss et al. 2002; Trapp 2006, Cohen et al. 2007). Due to these issues associated with modern reporting, combined with the large growth of reports (Weiss et al. 2002), the term

derecho has become outdated, as the definition was created when only the most severe MCSs received large amounts of damaging-wind reports. Nowadays, larger percentages of MCSs are associated with numerous reports, which can be misleading when trying to determine the true societal impact. Because of this, a joint effort between the National Severe Storms Laboratory and the Storm Prediction Center has begun in order to revise the definition of derecho to account for modern data. The updates include incorporating MCS structure and motion into the MCS-classification process. This paper specifically focuses on MCS motion, in terms of mean wind and propagation, and its relation to MCS organization/structure.

The physical structures of MCSs examined in this paper are features associated with severe-wind-producing MCSs. Key features include: the continuity/organization of the line of organized convection, which can gage the strength of the cold pool associated with an MCS; the presence, or absence, of a mesoscale convective vortex (MCV), which has been associated with derecho-producing MCSs (Wheatley and Trapp 2006; Metz and Bosart 2010); the appearance of the transition zone between the organized line of convection and the stratiform rain region; the angle between line orientation and mean wind, which can help provide insight as to the severe-weather threat (wind, flood, or both) associated with an MCS.

In this study, MCS motion is analyzed with a focus on mean wind, which is used as the advection component of motion, and propagation, which is any motion not accounted for by the mean wind. The focus is on mean wind and propagation because MCS motion is comprised of an advection component, which we calculated using mean wind, and a propagation component (Corfidi et al. 1996, Corfidi et al. 2003).

Mean wind has been determined in past MCS studies using the 850-300-mb winds. This approach gives equal weight to each pressure level in the atmosphere (Corfidi et al. 1996) and

results in a high correlation between MCS motion and the advection component of motion. The present study specifically investigates whether surface-6-kilometer mean winds or lifted condensation level (LCL) to equilibrium level (EL) mean winds best represent MCS motion. The mean wind values in this study, unlike in the 850-300 millibar (mb) calculation, are pressure weighted, which means that areas of the cloud with more mass make up a larger percentage of the mean wind calculation than layers with less mass.

Section 2 focuses on MCS case selection, how each MCS was classified, and the mathematical calculations performed. Section 3 focuses on the results and implications of the study, presented attribute by attribute, and section 4 summarizes the results of the study.

2. Methodology

a) Data collection

Using Storm Prediction Center (SPC) severe-wind reports, a collection of 357 severe-wind-producing warm-season (May-August) MCSs was created for the years 2010 to 2014. After the list of MCSs was compiled, each MCS was manually classified and tracked using NCDC national radar composite radar data (http://gis.ncdc.noaa.gov/map/viewer/#app=cdo). Each MCS was tracked 30-90 minutes within the mature phase along the organized line of convection. Features that were tracked varied depending on the shape and size of the MCS.

At the beginning of the tracking period, each MCS component was classified as meso-alpha scale (200-2000 km) or meso-beta scale (20-200 km) (Fig. 1) based on the spatial extent of the linear convection. If an MCS contained meso-alpha and meso-beta features, both features were tracked independently during an overlapping time period. Features tracked on the meso-alpha scale included areas of organized convection, middle of line segments, and the apex of

single arcing bows. Meso-beta scale features of interest included areas of organized convection, embedded bow echoes within a larger quasi-linear convective system (QLCS), small single-arcing bows and the middle of line segments. Start and end points were recorded for each meso-alpha or meso-beta feature via longitude and latitude coordinate documentation along with a corresponding start time and end time so that direction of movement, distance traveled and speed could be obtained for each MCS feature tracked. The direction of movement and speed are used to comprise the MCS motion vector for use in mathematical calculations.

Line orientation was tracked for each MCS during the mature phase and was measured at the angle relative to the meridian with no angle being greater than 90 degrees, clockwise rotation being positive and counterclockwise rotation being negative. This angle was measured precisely by taking two latitude and longitude points along the line orientation and calculating the angle between the line generated by the two points and a meridian intersecting that line. Each set of points were taken on a line tangent to the apex of a bow, parallel to the line segment, or line along the average orientation of a line segment with multiple large bow echoes within it.

The advection component of motion was determined at the beginning time and location of each MCS's starting point and included data of the pressure weighted mean wind in the surface-6-km layer and LCL-EL layer. The mean wind vector data came from the RUC/RAP data archived in the SPC Mesoanalysis data at the nearest grid point to the start point of each MCS at the beginning of closest hour to the start time. The winds before the start time are used since this best represents the near-storm environment prior to convective overturning.

b) Classification scheme

A subjective four-class scheme was created to group MCSs exhibiting similar structural characteristics. By grouping MCSs based on physical structures, it is possible to determine the relationship between the physical structure of MCSs and MCS motion, broken up by mean winds and propagation. The MCSs were all classified at the time of peak organization, with neither time period nor swath-length being considered.

Each class of MCS was based on differing physical features and levels of organization (Fig. 2). These different physical features can be attributed to strength of the cold pool, extent of large scale ascent in the synoptic environment, synoptic boundaries, remnant outflow boundaries, wind shear, as well as thermodynamic features such as the horizontal and vertical distribution of CAPE (Cohen et al. 2007).

"Class one" is composed of MCSs that are the best organized, contain a single arcing bow, have a well-defined mesoscale convective vortex (MCV) where the 40+dbz region coils at least 180 degrees from the leading convection to the stratiform rain region, and has a well formed transition zone between leading line of convection and the stratiform rain. The total number of class one systems is 15, for an average of three per year.

"Class two" is composed of MCSs that contain a single arcing bow, but do not exhibit a well-defined MCV. Class two is less organized than Class one. The total number of Class two systems is 88.

"Class three" is composed of MCSs that are not single arcing bows and may exhibit multiple arcing bows within the meso-alpha scale system, non-arcing line segments, and multiple large arcing bows. The total number of Class three systems is 201.

"Class four" is composed of MCSs that exhibit discontinuous 40-dbz reflectivity regions along the leading edge of convection and are the least organized of all MCSs. The total number of Class four systems is 53.

c) Calculations and statistical methods

The boxes used throughout the study represent the 25th, 50th, and 75th percentiles with the whiskers extend up to 1.5*IQR (inter-quartile range). Each whisker may extend up to 1.5*IQR, with outliers plotted beyond 1.5*IQR. All conclusions drawn from the box-and-whisker plots are from visual inspection of the distribution of data.

The box-and-whisker plots in this study that are broken up by class and distance and are color coded, with light grey representing "short" damage swath producing MCSs with damaging wind swaths less than 650 km. The medium grey represents MCSs with "long" swaths greater than or equal to 650 km. The dark grey represents all MCSs, short and long, for each class. The values given below each box-and-whisker plot represent the sample size in each plot.

As discussed earlier, surface-6-km winds and LCL-EL pressure-weighted mean winds were considered for use as the advection component for calculations used in this study. The analysis performed to determine which layer best represented MCS motion involved comparison of means, medians, interquartile ranges, and overall distributions by visual inspection. Two scatterplots were also used to help determine the layer of mean wind best represented MCS motion where MCS speed is plotted on the y-axis and the mean wind speed on the x-axis for each scatterplot. The corresponding correlation coefficients between mean wind speed and MCS speed are displayed below each graph in the results section.

Following the creation of the MCS motion vector, and determination of the advection component of motion vector, calculations were performed in order to calculate how speed of MCS motion differed from mean wind speed without taking direction into account. This was achieved by computing the magnitudes of the mean wind vector and MCS motion vector. The calculation in equation 1 provides the difference between mean wind speed ($\vec{A}$) and MCS speed ($\vec{M}$):

$$Difference = \left|\vec{M}\right| - \left|\vec{A}\right|. \quad (1)$$

We attribute MCS motion not associated with mean wind to a residual propagation vector. The propagation vector was calculated using equation 2 in Corfidi et al. (1995). The formula symbols used are as follows: "$\vec{M}$" represents MCS motion observed by radar, "$\vec{A}$" represents the advection component of MCS motion (mean wind) and "$\vec{P}$" represents the propagation vector:

$$\vec{M} = \vec{A} + \vec{P}. \quad (2)$$

Propagation, in the present study, is found by subtracting the mean wind vector from the MCS motion vector in equation 3:

$$\vec{P} = \vec{M} - \vec{A}. \quad (3)$$

Following the calculation of the propagation vector, the propagation vector was projected onto the mean wind vector in order to evaluate the amount of propagation in the direction of the mean wind in equation 4. This calculation is important due the magnitude of propagation being relatively large for strongly forced and back building MCSs, but not necessarily large in the direction of the mean wind. Using the projected component of the propagation vector onto the mean wind vector provides a better sense of how much additive motion along the mean wind is associated with propagation:

$$Comp\ _{\vec{A}}\vec{P} = \frac{\vec{A}\cdot\vec{P}}{|\vec{A}|}. \quad (4)$$

Lastly, the angle between line orientation and mean flow was determined. The angle was computed by measuring the acute angle between the intersection of the mean wind vector and the line orientation. This results in angles being no greater than 90 degrees.

3. Results

a) Surface-6-km mean winds vs LCL-EL mean winds

As stated earlier, two different layers of the atmosphere were considered for use as the mean wind vector. Previous MCS studies have used 850-300-mb non-pressure-weighted winds as the mean wind vector (Corfidi et al 1995; Corfidi et al 2003). However, this study investigated the layers surface-6 km and LCL-EL since these layers represent a comprehensive coverage of the cloud layer.

After analyzing Fig. 3, a connection between mean wind magnitude and MCS motion magnitude can be made. Surface-6-km mean wind magnitude was found to have a correlation coefficient of 0.52 when compared with magnitude of MCS motion, while LCL-EL has a coefficient of over 0.54. After the correlation between MCS motion and mean wind is made, results presented in Fig. 4 then show the LCL-EL mean wind speed better represents MCS speed as the distribution of data resembles MCS alpha and beta speed much closer than the surface-6-km distribution.

Although the findings in this study show LCL-EL to be a more accurate representation of MCS speed than the surface-6-km layer, it has not been determined whether the LCL-EL layer best represents MCS motion compared to other layers. In previous studies, the mean wind was taken from 850-300 mb and was found to have a higher correlation coefficient than LCL-EL in

this study, however none of the previous studies have compared the 850-300-mb layer to the layers used in this study. To determine whether 850-300 mb is truly a better representation of MCS motion a study would need to compare the layer directly to the LCL-EL layer with the same test group of MCS speed values to make such a conclusion.

b) Magnitude of MCS motion

After determining the mean wind vector used for the rest of the calculations to be LCL-EL pressure weighted mean winds, the speed of each class of MCS was plotted (Fig. 5). This was calculated by taking the magnitude of the MCS motion vector, which represents the speed of each MCS.

It was found that Class one systems generally moved at a higher speed than any other class of MCS. It also can be noted that Class two systems generally moved faster than Class three and Class four systems as well. This signals that MCS organization may be related to MCS speed, with this especially being true for MCSs with single arcing bows.

c) Mean wind speed by class

Observing that each class of MCS differs in speed, it was inspected whether the difference in speed could be associated with mean wind variations between classes or propagation differences between classes, knowing that MCS motion is comprised of an advection component and a propagation component. Using the LCL-EL mean winds as the advection component, a relationship between the magnitude of mean wind and class and length was investigated. It was thought that perhaps the mean wind speed could have been a defining attribute in the speed of MCS motion. However, there was no obvious relationship found

between mean wind speed and MCS speed. The results in Fig. 6 show a nearly identical distribution of mean winds for all classes. This suggests that mean winds cannot be associated with the differences in MCS speed.

d) Difference between MCS speed and mean wind speed

The difference between MCS speed and mean wind speed was calculated following the mean wind distribution findings, in which mean wind speed was directly subtracted out of MCS speed. The resulting distribution shown in Fig. 7 demonstrates that there is a difference between mean wind speed and MCS speed, with Class one systems moving faster than any other system.

e) Magnitude of propagation

The magnitude of propagation (determined by subtracting the mean wind vector from the MCS motion vector) yielded results that demonstrated the difference in motion is associated with differing propagation values between classes.

Figure 8 indicates that the magnitude of propagation was largest for Class one MCSs followed, in sequence, by the other three classes. The apparent relationship between the magnitude of propagation and class ranking suggests that the level of organization and physical appearance of a MCS on WSR-88D provides guidance as to the influences of propagation on overall MCS motion. Class one and Class two, the most organized of all MCSs, have the most propagation while Class three and Class four, are the least organized of all MCSs and have lesser magnitudes of propagation.

f) Projection of propagation onto the mean wind vector

The propagation in the direction of mean wind was calculated by taking the component of projection of the propagation vector onto the mean wind vector, with the results shown in Fig. 9. The highest positive component of projection in Class one systems means that propagation is in the direction of mean wind. This implies that propagation added motion in the direction of the mean wind, resulting in Class one systems having higher speeds than any other class. Furthermore, the fact that propagation was in the same direction as mean wind suggests that the cold pool in Class one systems tended to elongate in the direction of the mean wind more so than in any other class. The elongation in the same direction of the mean wind led to new cell development along gust front, which increased forward motion relative to the mean flow.

g) Angle between the mean wind vector and line orientation

To investigate whether it is true that the cold pool elongated in the direction of the mean winds, the angle between line orientations was computed. This calculation helps provide insight as to how the mean winds could have affected MCS motion, with the expectation being that faster moving systems being oriented more perpendicular to the mean wind. The results are shown in Fig. 10.

This distribution revealed that class one systems have the largest angle between the mean wind vector and line orientation. This means that in these cases the line orientation of the line of convection was more perpendicular to the mean wind vector. This finding confirms that systems in which the convection is oriented at a greater angle to the mean wind vector gain forward speed, likely due to elongation of the cold pool in the direction of the mean winds, compared to systems that align more parallel to the mean wind.

4. Summary

The relationship between physical structure of MCSs and MCS motion was investigated with the study of 357 warm season, damaging-wind-producing MCSs between the years 2010-2014. A trackable feature, such as an area of organized convection, middle of a line segment, or apex of a bow, was tracked manually for 30-90 minutes within the mature phase using the NCDC national mosaic radar. From the data collected, the MCS motion vector was determined, then the mean winds in the layers surface-6-km and LCL-EL were investigated to determine which layer best represented MCS motion. Following the mean wind layer calculation, the propagation magnitude, projection of propagation onto the mean wind vector, and the angle between line orientation and mean wind were calculated.

It was determined that the pressure-weighted winds in the LCL-EL layer best represented MCS motion compared to the surface-6-km layer. From that initial finding it was determined that Class one systems were the best organized consisting of a well defined MCV and transition zone, and had the highest speed, highest magnitude of propagation, most propagation in the direction of the mean wind, and largest angle between line orientation and the mean wind vector.

The findings show that the difference in speed between classes was attributed to different propagation vectors, since the mean wind distribution was similar for each for class. These findings suggest that the most organized MCSs tend to move the fastest, in association with additive effects of propagation, and orient most orthogonally to the mean winds. This helps explain the tendency for organized MCSs, specifically those in Class one, to produce damaging winds. The elongation of the cold pool adds forward motion in the same direction as the mean wind vector and combination results in stronger surface winds and faster forward motion.

Appendix

Procedure for calculating advection component of motion and propagation

Radar data are provided by NCDC national composite radar. Mean wind data are provided by the Storm Prediction Center RUC/RAP-based Mesoanalysis system. Pressure-weighted mean winds in the layers surface-6 km and LCL-EL were inspected, and LCL-EL wind speed data distribution best matched MCS speed data distribution. LCL-EL mean winds where selected as the advection component of motion. Propagation accounted for any residual values in the MCS motion equation in Corfidi et al (1996).

Acknowledgements

NCDC National Composite Mosaic Radar for providing radar images used in this study, Patrick Marsh for instruction on programming, Israel Jirak for presentation review, James Correia for practice talk review, Massey Bartolini for instruction on programming, Tomer Burg for instruction on programming, and Kyle Pallozzi for presentation review.

This work was prepared by the authors with funding provided by National Science Foundation Grant No. AGS-1062932, and NOAA/Office of Oceanic and Atmospheric Research under NOAA-University of Oklahoma Cooperative Agreement #NA11OAR4320072, U.S. Department of Commerce. The statements, findings, conclusions, and recommendations are those of the author(s) and do not necessarily reflect the views of the National Science Foundation, NOAA, or the U.S. Department of Commerce.

References

Ashley, W. S., and T. L. Mote, 2005: Derecho hazards in the Unites States. *Bull. Amer. Soc.,* **86,** 1577-1592.

Cohen, A. E., 2007: Discrimination of Mesoscale Convective System Environments Using Sounding Observations. *Wea. Forecasting,* **22,** 1045-1062.

Corfidi, S. F., 1996: Predicting the Movement of Mesoscale Convective Complexes. *Wea. Forecasting,* **11,** 41-46.

Corfidi, S. F., 2003: Cold Pools and MCS propagation: Forecasting the motion of downwind-developing MCSs. *Wea. Forecasting,* **18,** 997-1017.

Doswell, C. A III, 1996: Flash Flood Forecasting: An Ingredients-Based Methodology. *Wea. Forecasting,* **11,** 560-581.

Fritsch, J.M., 1986: The contribution of mesoscale convective weather systems to the warm-season precipitation in the United States. *J. Climate Appl. Meteor.,* **25,** 1333-1345.

Jirak, I. L, and W. R. Cotton, 2007: Observational Analysis and the Predictability of Mesoscale Convective Systems. *Wea. Forecasting,* **22,** 813-838.

Maddox, R. A., 1980: Mesoscale Convective Complexes. *Bull. Amer. Meteor. Soc.,* **61,** 1374-1387.

Metz, N. D, and L. F. Bosart, 2010: Derecho and MCS development, evolution, and multiscale interactions during 3-5 July 2003. *Mon. Wea. Rev.,* **138,** 3048-3070.

Parker, M. D., and R. H. Johnson, 2000: Organizational modes of midlatitude mesoscale convective systems. *Mon. Wea. Rev.,* **128,** 3413-3436.

Trapp, R. J., 2006: Buyer beware: Some words of caution on the use of severe wind reports in post-event assessment and research. *Wea. Forecasting,* **21,** 408-415.

Weiss, S. J., J. A. Hart, and P. R. Janish, 2002: An examination of severe thunderstorm wind report climatology: 1970-1999. Preprints, *21st Conf. on Severe Local Storms,* San Antonio, TX, Amer. Meteor. Soc., CD-ROM, 11B2.

Wheatley, D. M., and R. J. Trapp, 2006: Radar and damage analysis of severe bow echoes observed during BAMEX. *Mon. Wea. Review,* **134,** 791-806.

Figure Captions

FIG. 1. Example of (a) Meso-alpha scale MCS with leading line of convection between 200-2000 km, (b) and meso-beta scale MCS with leading line of convection between 20-200 km, and (c) and meso-alpha scale MCS with meso-beta scale features.

FIG. 2. Examples of all four class are shown: (a) “Class one” MCS, (b) “Class two” MCS, (c) “Class three” MCS, and (d) “Class four” MCS.

FIG. 3. (a) Plot of LCL-EL mean wind speed (knots) on the x-axis, MCS speed (knots) on the y-axis and correlation coefficient between mean wind speed and MCS speed. (b) Plot of the surface-6-km mean wind speed (knots) on the x-axis, MCS speed (knots) on the y-axis and correlation coefficient between mean wind speed and MCS speed.

FIG. 4. Box and whisker plots representing meso-alpha scale speed, meso-beta scale speed, surface-6-km mean wind speed, LCL-EL mean wind speed. Boxes represent 25th, 50th, and 75th percentiles. Whiskers extend up to 1.5*IQR (interquartile range). Pluses represents outliers in the data.

FIG. 5. Box and whisker plots broken up by class and damage swath length. The light grey represents “short” damage swaths less than 650 km, medium grey represents “long” damage swaths greater than or equal to 650 km, and dark grey represents all MCSs of each class, including both “short” and “long” damage swaths.

FIG. 6. The magnitude of mean wind (mean wind speed), is plotted with MCSs broken up by class and distance.

FIG. 7. MCS Speed minus mean wind speed for MCSs is plotted with MCSs broken up by class and distance.

FIG. 8. Magnitude of MCS propagation is plotted with MCSs broken up by class and distance.

FIG. 9. The values for the component of the propagation vector projected onto the mean wind vector are plotted with MCSs broken up by class and distance.

FIG.10. The acute angle between the intersection of the mean wind vector and line orientation is plotted with MCSs broken up by class and distance.

Figures

(a)

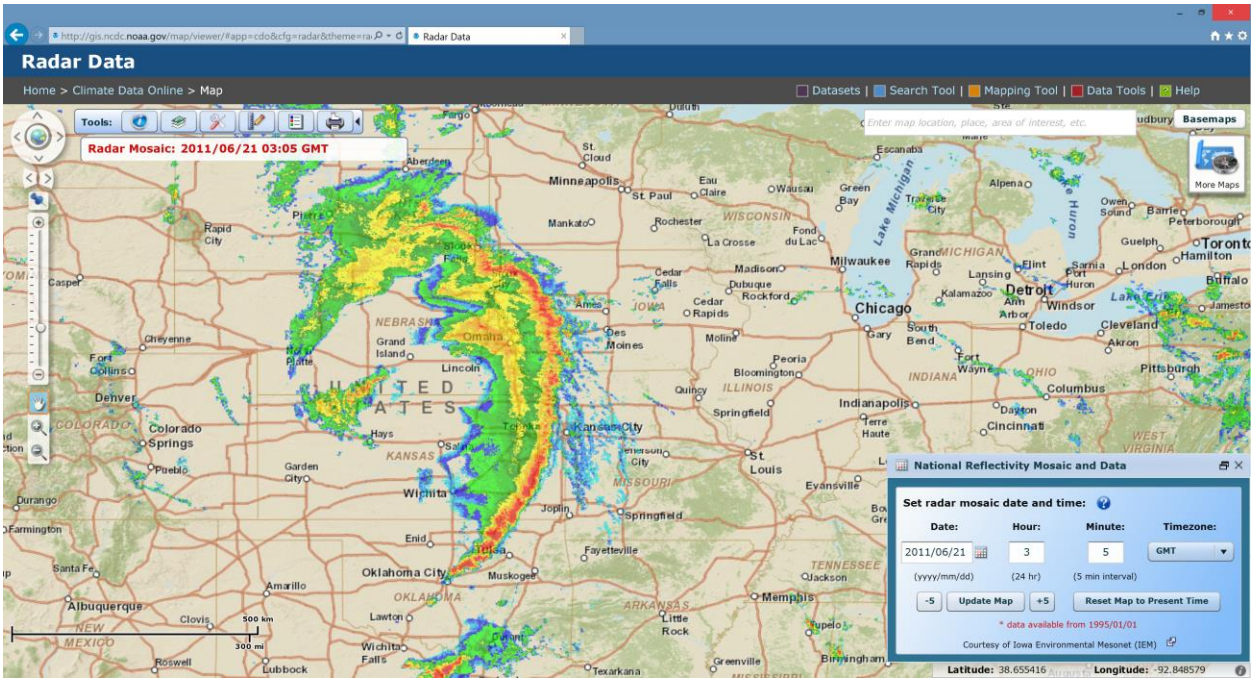
Radar Data
Home > Climate Data Online > Map
Datasets | Search Tool | Mapping Tool | Data Tools | Help
Tools:
Radar Mosaic: 2011/06/21 03:05 GMT
Basemaps
More Maps
National Reflectivity Mosaic and Data
Set radar mosaic date and time:
Date: 2011/06/21
Hour: 3
Minute: 5
Timezone: GMT
(yyyy/mm/dd)
(24 hr)
(5 min interval)
-5
Update Map
+5
Reset Map to Present Time
* data available from 1995/01/01
Courtesy of Iowa Environmental Mesonet (IEM)
Latitude: 38.655416
Longitude: -92.848579

(b)

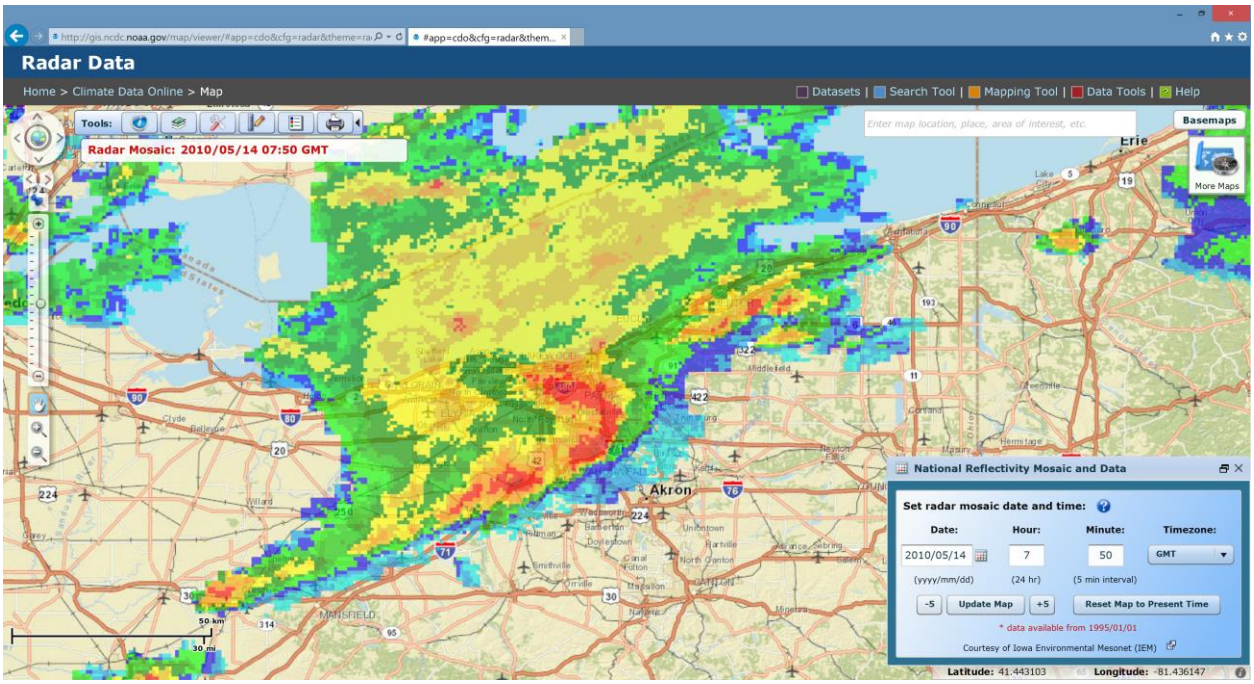
Radar Data
Home > Climate Data Online > Map
Datasets | Search Tool | Mapping Tool | Data Tools | Help
Tools:
Radar Mosaic: 2010/05/14 07:50 GMT
Basemaps
More Maps
National Reflectivity Mosaic and Data
Set radar mosaic date and time:
Date: 2010/05/14
Hour: 7
Minute: 50
Timezone: GMT
(yyyy/mm/dd)
(24 hr)
(5 min interval)
-5
Update Map
+5
Reset Map to Present Time
* data available from 1995/01/01
Courtesy of Iowa Environmental Mesonet (IEM)
Latitude: 41.443103
Longitude: -81.436147

(c)

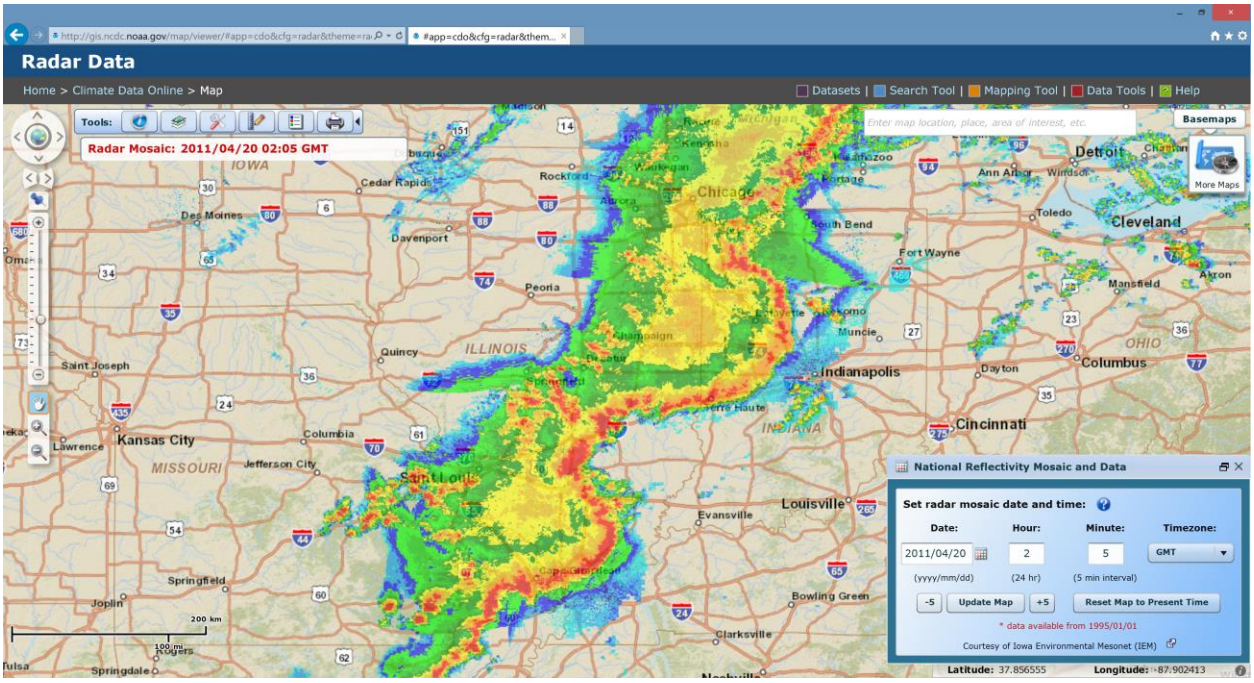

FIG. 1. Example of (a) Meso-alpha scale MCS with leading line of convection between 200-2000 km, (b) and meso-beta scale MCS with leading line of convection between 20-200 km, and (c) and meso-alpha scale MCS with meso-beta scale features.

(a)

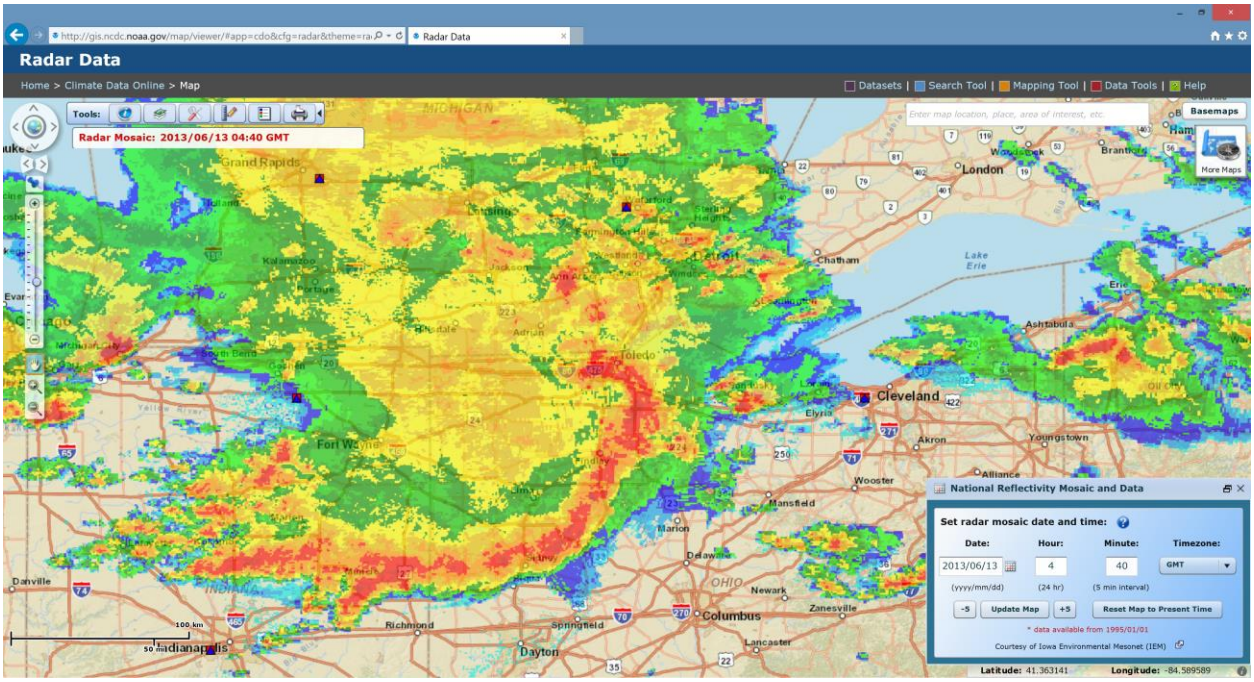
Radar Data
Home > Climate Data Online > Map
Datasets | Search Tool | Mapping Tool | Data Tools | Help
Radar Mosaic: 2013/06/13 04:40 GMT
Basemaps
More Maps
National Reflectivity Mosaic and Data
Set radar mosaic date and time:
Date:
Hour:
Minute:
Timezone:
2013/06/13
4
40
GMT
(yyyy/mm/dd)
(24 hr)
(5 min interval)
-5
Update Map
+5
Reset Map to Present Time
* data available from 1995/01/01
Courtesy of Iowa Environmental Mesonet (IEM)
Latitude: 41.363141
Longitude: -84.589589
Cleveland
Columbus
Dayton
Toledo
Detroit
Chicago
Indianapolis
Fort Wayne
Akron
Youngstown
London
Mansfield
Wooster
Lake Erie
OHIO
MICHIGAN

(b)

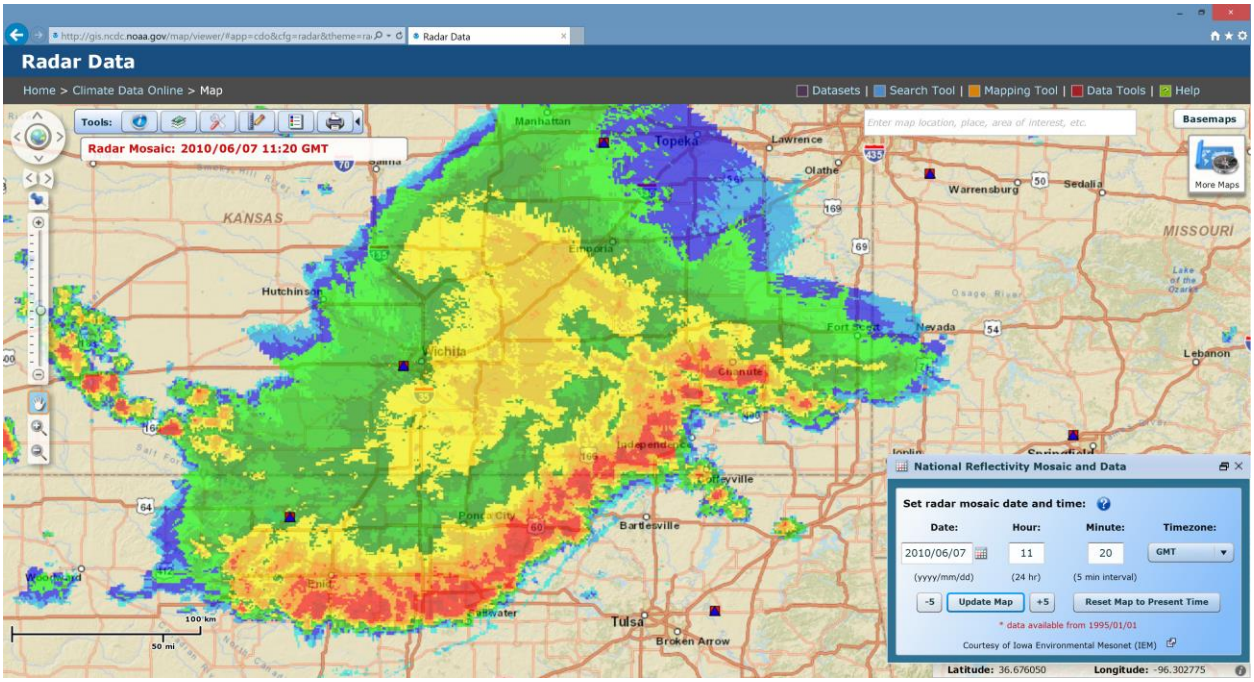
Radar Data
Home > Climate Data Online > Map
Datasets | Search Tool | Mapping Tool | Data Tools | Help
Radar Mosaic: 2010/06/07 11:20 GMT
Basemaps
More Maps
National Reflectivity Mosaic and Data
Set radar mosaic date and time:
Date:
Hour:
Minute:
Timezone:
2010/06/07
11
20
GMT
(yyyy/mm/dd)
(24 hr)
(5 min interval)
-5
Update Map
+5
Reset Map to Present Time
* data available from 1995/01/01
Courtesy of Iowa Environmental Mesonet (IEM)
Latitude: 36.676050
Longitude: -96.302775
Topeka
Wichita
Tulsa
Broken Arrow
Bartlesville
Nevada
Lebanon
Warrensburg
Sedalia
Olathe
Lawrence
Manhattan
Hutchinson
Emporia
KANSAS
MISSOURI

(c)

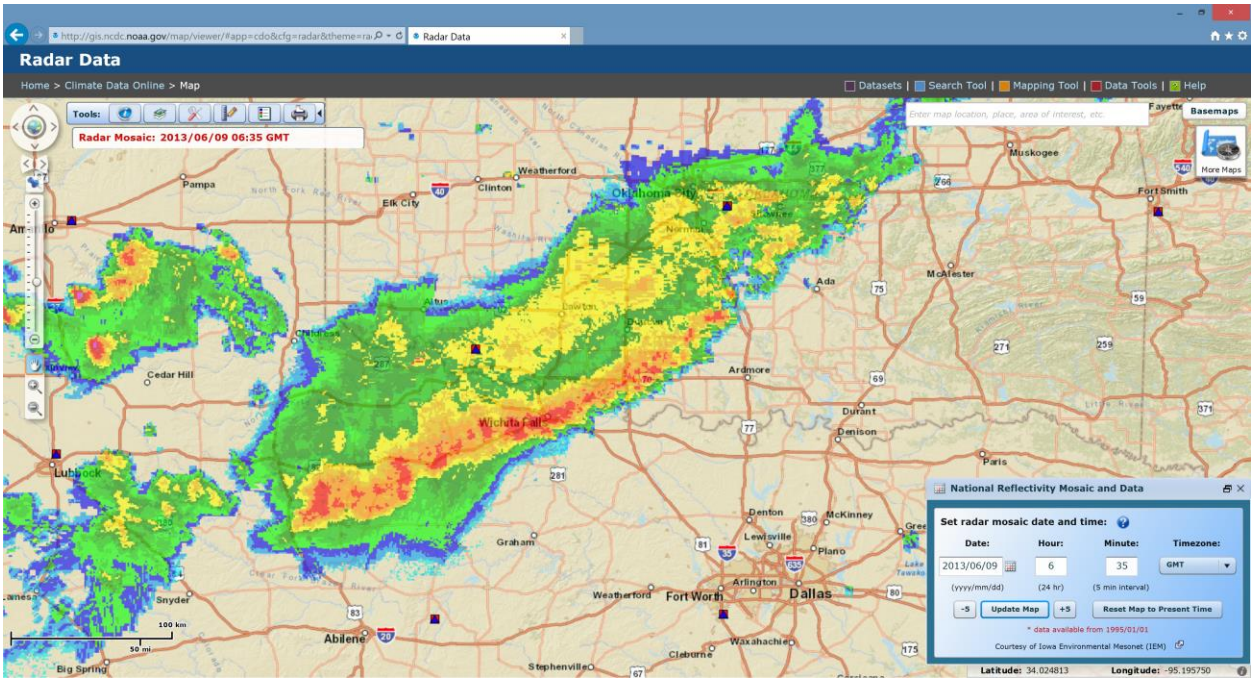

(d)

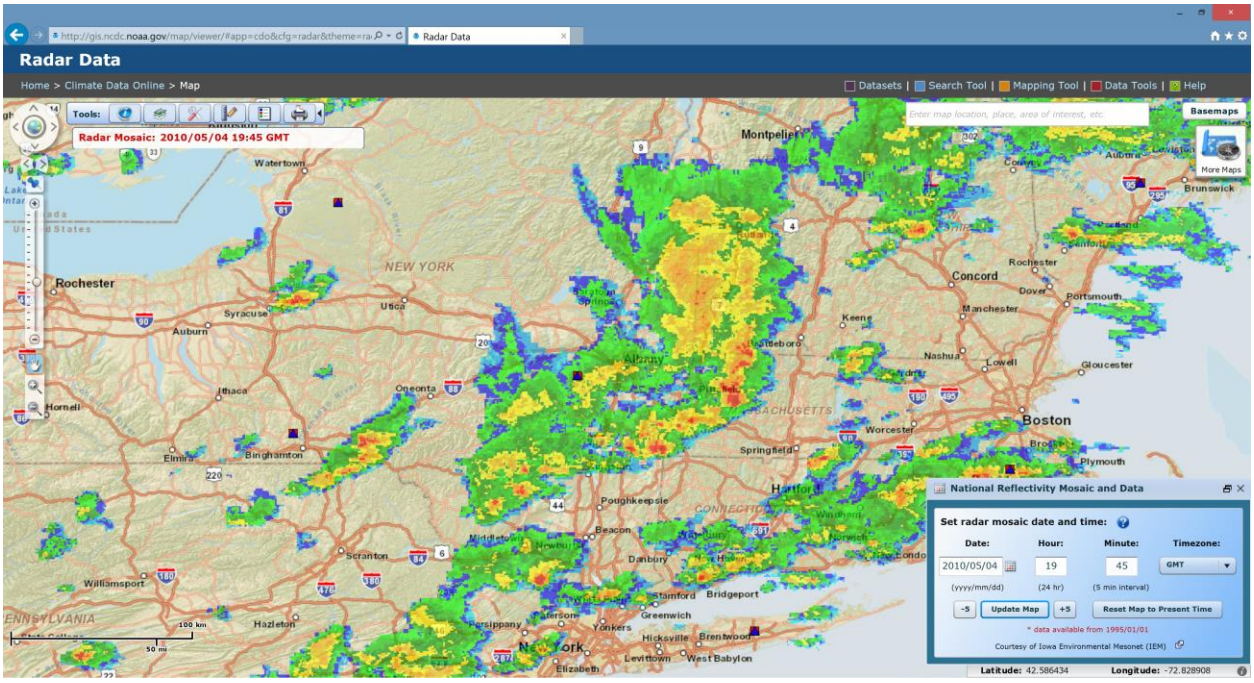

FIG. 2. Examples of all four class are shown: (a) “Class one” MCS, (b) “Class two” MCS, (c) “Class three” MCS, and (d) “Class four” MCS.

(a)

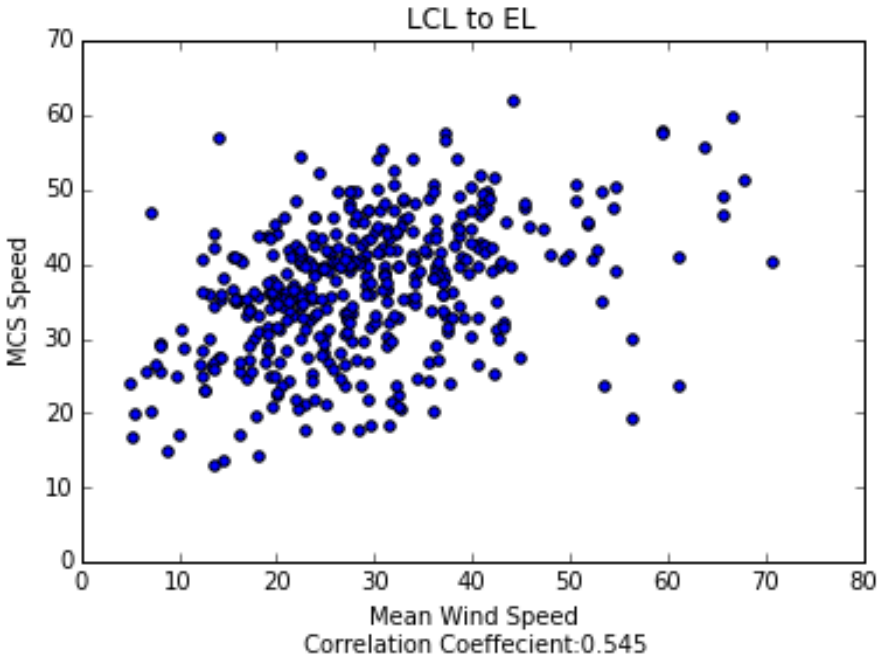
LCL to EL
MCS Speed
Mean Wind Speed
Correlation Coeffecient:0.545

(b)

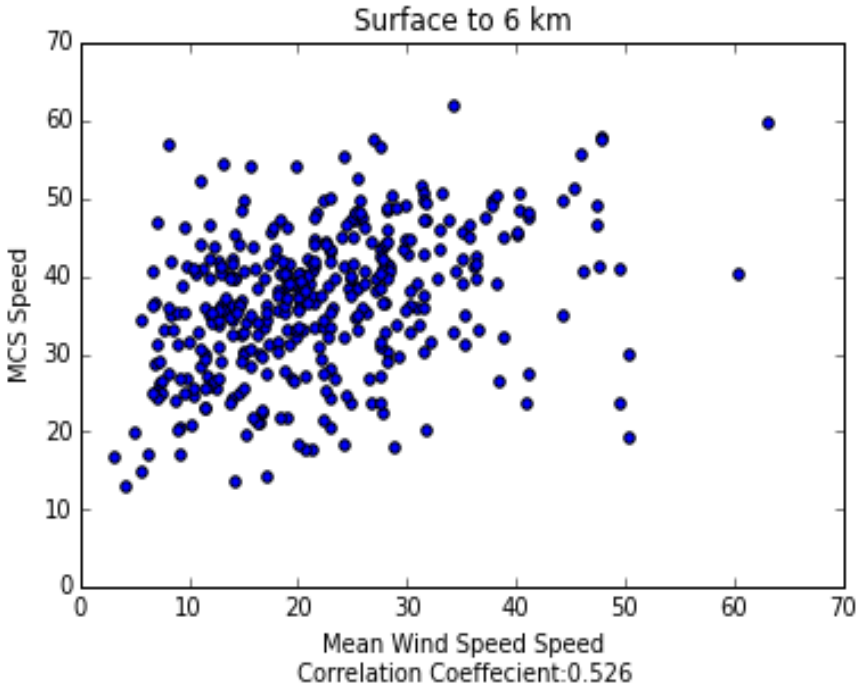
Surface to 6 km
MCS Speed
Mean Wind Speed Speed
Correlation Coeffecient:0.526

FIG. 3. (a) Plot of LCL-EL mean wind speed (knots) on the x-axis, MCS speed (knots) on the y-axis and correlation coefficient between mean wind speed and MCS speed. (b) Plot of the surface-6-km mean wind speed (knots) on the x-axis, MCS speed (knots) on the y-axis and correlation coefficient between mean wind speed and MCS speed.

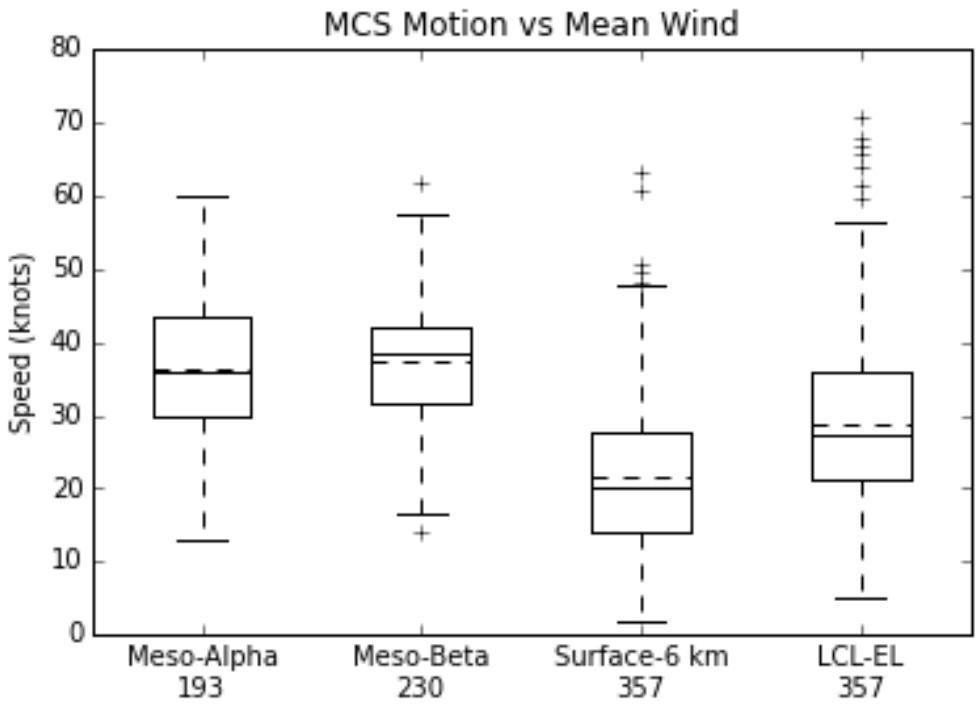

FIG. 4. Box and whisker plots representing meso-alpha scale speed, meso-beta scale speed, surface-6-km mean wind speed, LCL-EL mean wind speed. Boxes represent 25th, 50th, and 75th percentiles. Whiskers extend up to 1.5*IQR (interquartile range). Pluses represents outliers in the data.

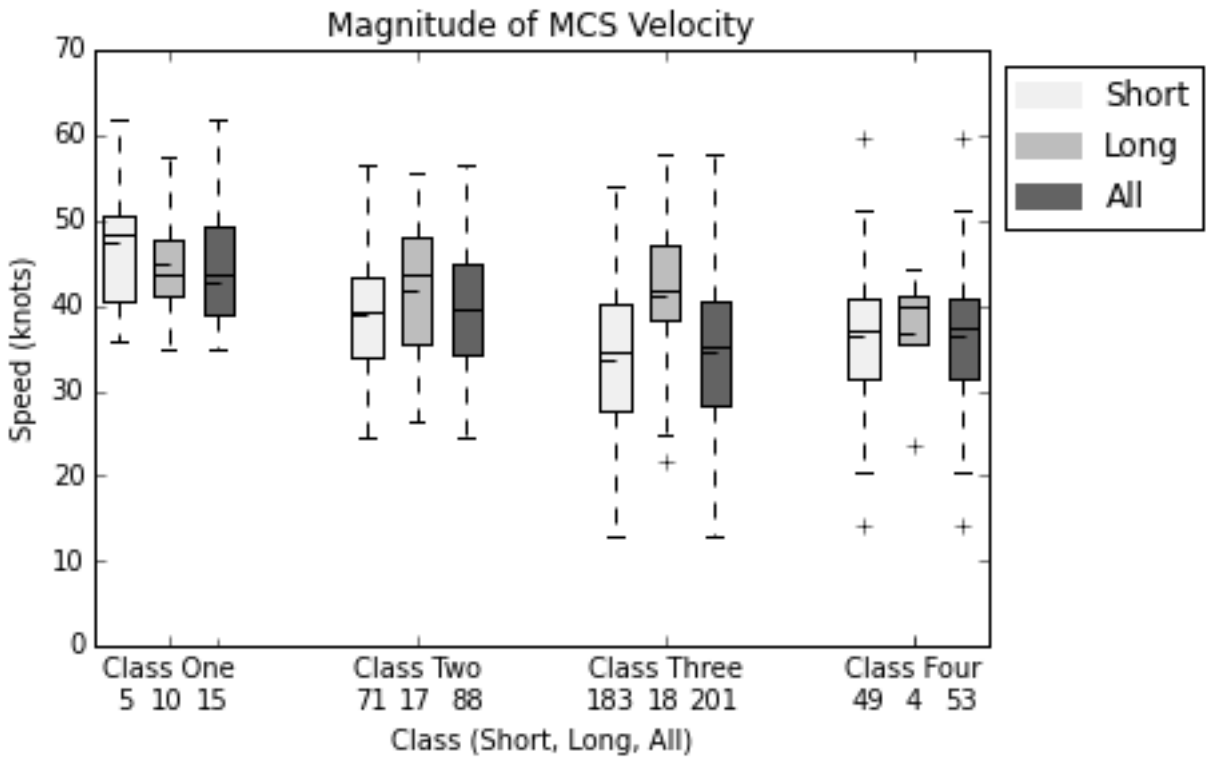

FIG. 5. Box and whisker plots broken up by class and damage swath length. The light grey represents "short" damage swaths less than 650 km, medium grey represents "long" damage swaths greater than or equal to 650 km, and dark grey represents all MCSs of each class, including both "short" and "long" damage swaths.

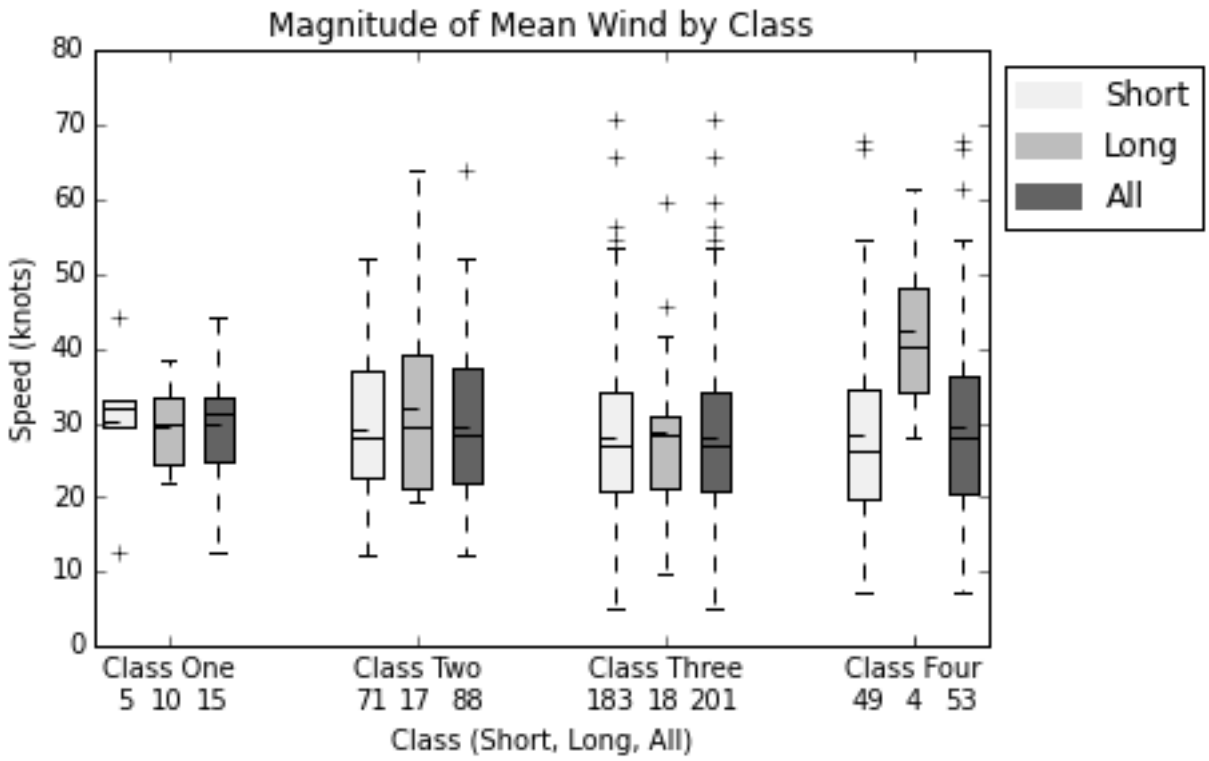

FIG. 6. The magnitude of mean wind (mean wind speed), is plotted with MCSs broken up by class and distance.

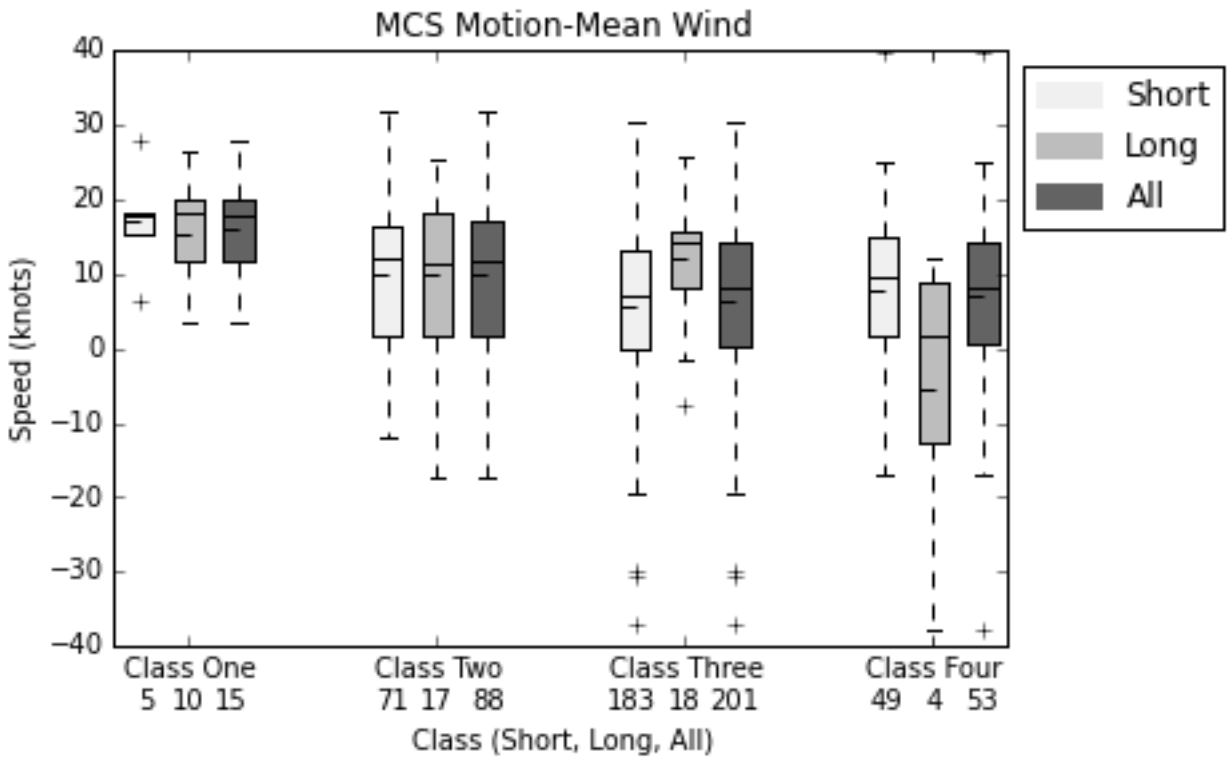

FIG. 7. MCS Speed minus mean wind speed for MCSs is plotted with MCSs broken up by class and distance.

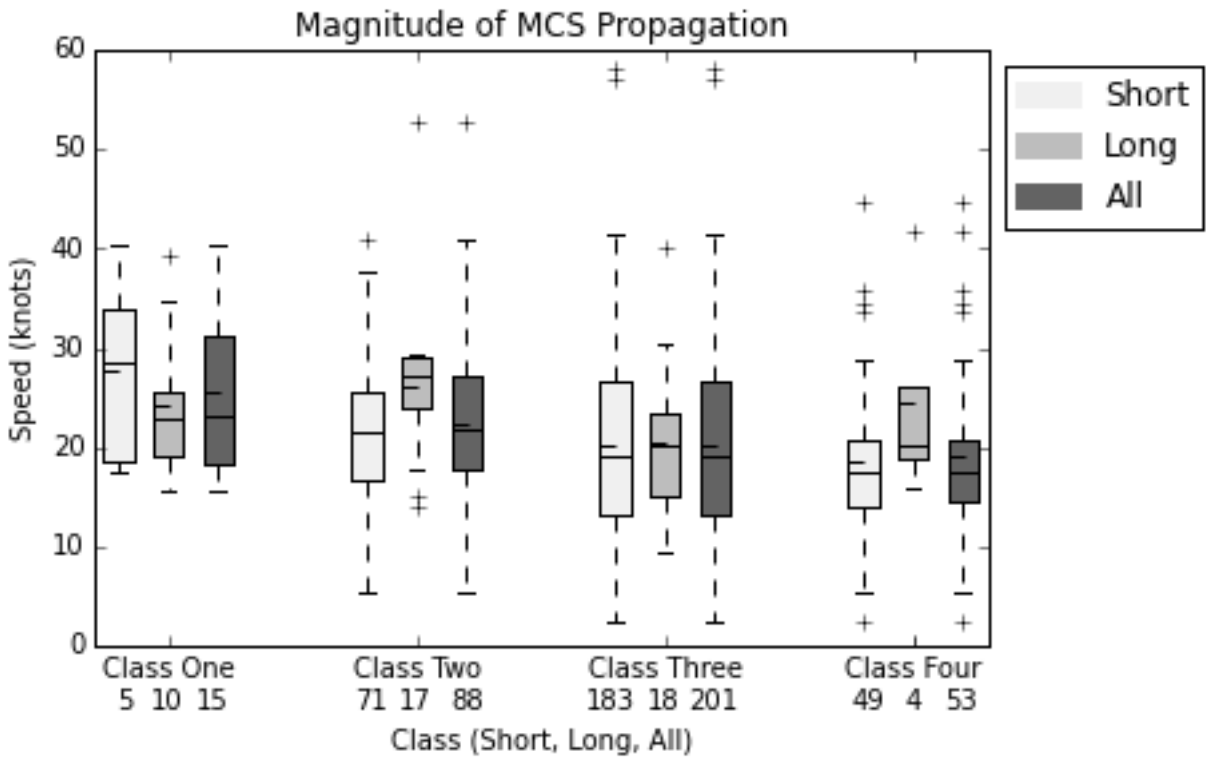

FIG. 8. Magnitude of MCS propagation is plotted with MCSs broken up by class and distance.

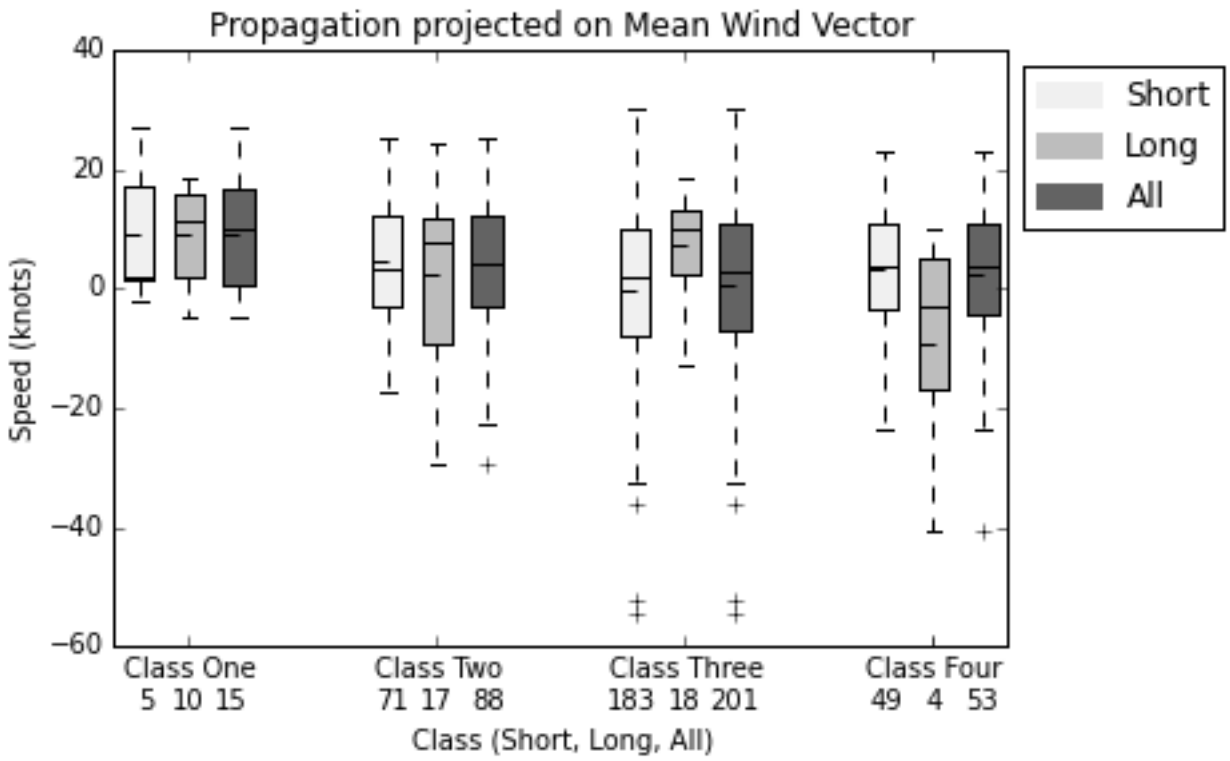

FIG. 9. The values for the component of the propagation vector projected onto the mean wind vector are plotted with MCSs broken up by class and distance.

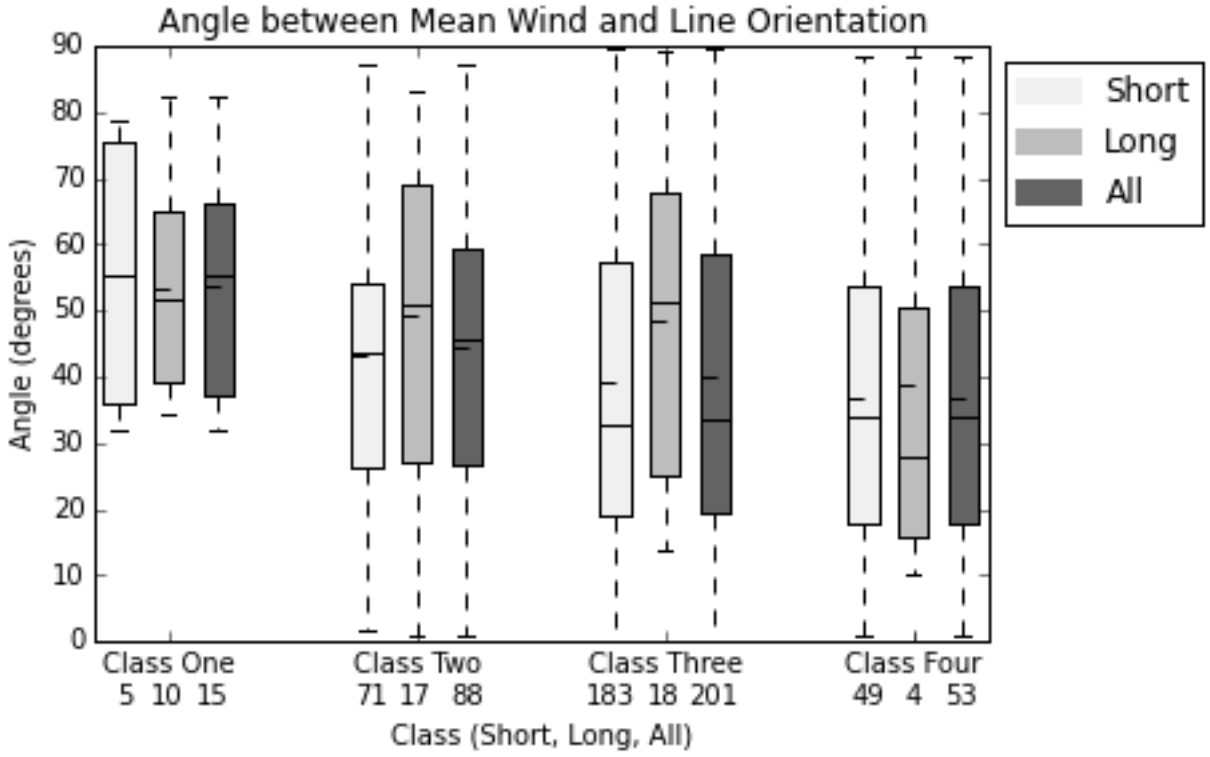

FIG.10. The acute angle between the intersection of the mean wind vector and line orientation is plotted with MCSs broken up by class and distance.